Quantization of a Billiard Model for Interacting Particles

Thomas Papenbrock* and Tomaž Prosen†
Centro Internacional de Ciencias A.C., 62131 Cuernavaca, Mexico
(Received 6 May 1999)

We consider a billiard model of a self-bound, interacting three-body system in two spatial dimensions. Numerical studies show that the classical dynamics is chaotic. The corresponding quantum system displays spectral fluctuations that exhibit small deviations from random matrix theory predictions. These can be understood in terms of a new type of scarring caused by a one-parameter family of orbits inside the collinear manifold.

PACS numbers: 05.45.Mt, 03.65.Ge, 03.65.Sq

The field of quantum chaos has reached a mature state for two-dimensional systems. It is well known that quantum spectra and wave functions of classically chaotic systems exhibit universal properties (e.g., spectral fluctuations) [1] as well as deviations (e.g., scars of periodic orbits) [2,3] when compared to random matrix theory (RMT) predictions of the Gaussian orthogonal ensemble (GOE). Recent experimental and theoretical efforts aim at the investigation of chaos in higher dimensional systems. As examples, we mention experiments in elastomechanics [4], physics of resonant cavities [5], the first quantizations of three-dimensional billiards [6,7], the construction of high-dimensional chaotic billiards with no dispersing elements [8], and chaos in many-body systems [9]. The study of such systems is interesting because their phase space structure is much richer than that of two-dimensional ones, and qualitatively new features appear. In particular, invariant manifolds in billiards [7] and systems of identical particles [10] may lead to an enhancement in the amplitude of wave functions [11,12] provided that classical motion is not too unstable in their vicinities.

It is the purpose of this Letter to investigate a new type of wave function scarring in an interacting self-bound few-body system. We choose a model system that is realized as a convex billiard with no dispersing elements. This model system turns out to be simple enough to be understood in classical and quantum mechanics, yet it captures the important feature of self-bound many-body systems: an attractive two-body force.

This Letter is organized as follows. First we study the classical dynamics of our billiard model. Second, we compute highly excited eigenstates of the corresponding quantum system and compare the results with RMT predictions.

Recently, a self-bound many-body system realized as a billiard has been proposed in the framework of nuclear physics [13]. Let us consider the corresponding three-body system with the Hamiltonian

$$H = \sum_{i=1}^{3} \frac{\vec{p}_i^{\,2}}{2m} + \sum_{i<j} V(|\vec{r}_i - \vec{r}_j|), \tag{1}$$

where $\vec{r}_i$ is a two-dimensional position vector of the ith particle and $\vec{p}_i$ is its conjugate momentum. The two-body potential is

$$V(r) = \begin{cases} 0 & \text{for } r < a \\ \infty & \text{for } r \geq a\,. \end{cases} \tag{2}$$

The particles thus move freely within a convex billiard in six-dimensional configuration space and undergo elastic reflections at the walls. Besides the energy E, the total momentum $\vec{P}$ and angular momentum L are conserved quantities which leave us with three degrees of freedom. In what follows we consider the case $\vec{P} = 0, L = 0$.

To study the classical dynamics it is convenient to fix the velocity $\vec{v}_1^{\,2} + \vec{v}_2^{\,2} + \vec{v}_3^{\,2} = 1$. We want to compute the Lyapunov exponents of several trajectories. To this purpose we draw initial conditions at random and compute the tangent map [14] while following their time evolution. To ensure good statistics and good convergence, we follow an ensemble of 7×10^4 trajectories for 10^5 bounces off the boundary. All followed trajectories have positive Lyapunov exponents. The ensemble averaged value of the maximal Lyapunov exponent and its rms deviation are $\lambda a = 0.3933 \pm 0.0015$, while the second Lyapunov exponent is also always positive. Thus, the system is chaotic for practical purposes. However, we have no general proof that no stable orbits exist. The reliability of the numerical computation was checked by (i) comparing forward with backward evolution, (ii) observing that energy, total momentum, and angular momentum are conserved to high accuracy during the evolution, and (iii) using an alternative method [15] to determine the Lyapunov exponent.

The considered billiard possesses two low-dimensional invariant manifolds that correspond to symmetry planes. The first "collinear" manifold is defined by configurations where all three particles move on a line. The dynamics inside this manifold is governed by the one-dimensional analog of Hamiltonian (1). After separation of the center-of-mass motion, one obtains a two-dimensional billiard with the shape of a regular hexagon. This system is known to be *pseudointegrable* [16]. To study the motion in the vicinity of the collinear manifold, we compute the *full phase space* stability matrix for several periodic orbits inside the collinear manifold which come in one-dimensional families and can be systematically enumerated using the tiling property of the hexagon. All considered types of orbits *except two* are unstable in the *transverse* direction: (i) The family of *bouncing ball* orbits (i.e. two particles bouncing, the third one at rest in between) is marginally stable (parabolic) in full phase space. (ii) The family of orbits depicted in Fig. 1 is stable (elliptic) in two *transversal* directions and marginally stable (parabolic) in the other 10 directions of 12-dimensional phase space. Though this behavior does not spoil the ergodicity of the billiard, one may expect that it causes the quantum system to display deviations from RMT predictions. Note that this family of periodic orbits differs from the bouncing ball orbits which have been extensively studied in two- and three-dimensional billiards [6,17] since (i) it is restricted to a lower dimensional invariant manifold, and (ii) it is elliptic (complex unimodular pair of eigenvalues) in one conjugate pair of directions.

The second invariant manifold is defined by those configurations where two particles are mirror images of each other while the third particle is restricted to the motion on the (arbitrarily chosen) symmetry line. Inside this manifold, one finds partly regular and partly chaotic dynamics. However, the motion is infinitely unstable in the transverse direction due to nonregularizable three-body collisions.

The quantum mechanics is done using the coordinates

$$\begin{aligned} \vec{x} &= (\vec{r}_1 + \vec{r}_2 + \vec{r}_3)/\sqrt{3}, \\ \rho \cos\frac{\theta'}{2}\begin{pmatrix}\cos(\phi - \varphi'/2)\\ \sin(\phi - \varphi'/2)\end{pmatrix} &= (\vec{r}_1 - \vec{r}_2)/\sqrt{2}, \qquad (3) \\ \rho \sin\frac{\theta'}{2}\begin{pmatrix}\cos(\phi + \varphi'/2)\\ \sin(\phi + \varphi'/2)\end{pmatrix} &= (\vec{r}_1 - \vec{r}_2 - 2\vec{r}_3)/\sqrt{6}, \end{aligned}$$

Here ρ, θ', and φ' describe the intrinsic motion of the three-body system while $\vec{x}$ and ϕ are the center of mass and the global orientation, respectively. In a second transformation we apply a rotation of $\pi/2$ around the abscissa corresponding to spherical coordinates $(\rho, \theta', \varphi')$, namely, $\tan\varphi = -\cot\theta'/\cos\varphi'$ and $\cos\theta = \sin\theta'\sin\varphi'$ and obtain for the Laplacian in the subspace $\vec{P} = 0, L = 0$,

$$\Delta = \frac{\partial^2}{\partial\rho^2} + \frac{3}{\rho}\frac{\partial}{\partial\rho} + \frac{4}{\rho^2}\left[\frac{\partial^2}{\partial\theta^2} + \cot\theta\frac{\partial}{\partial\theta} + \frac{1}{\sin^2\theta}\frac{\partial^2}{\partial\varphi^2}\right]. \qquad (4)$$

Products of Bessel functions and spherical harmonics,

$$\psi_{k,l,l_z}(\rho,\theta,\varphi) = (k\rho)^{-1}J_{2l+1}(k\rho)Y_l^{l_z}(\theta,\varphi), \qquad (5)$$

are eigenfunctions of the Laplacian (4), i.e., $\Delta\psi_{k,l,l_z}(\rho,\theta,\varphi) = -k^2\psi_{k,l,l_z}(\rho,\theta,\varphi)$ with the usual relation between wave vector and energy $k = \hbar^{-1}(2mE)^{1/2}$. Figure 2 shows a picture of the billiard taking (ρ,θ,φ) as spherical coordinates. The billiard possesses a D_{3h} symmetry. In the fundamental domain $(\theta,\varphi) \in (0,\pi/2) \times (-\pi/6,\pi/6)$ the boundary is given by

$$\rho_B(\theta,\varphi) = a[1 + \sin\theta\sin(\varphi + \pi/3)]^{-1/2}. \qquad (6)$$

The collinear manifold is the equatorial plane $\theta = \pi/2$. The second invariant manifold is given by the vertical symmetry planes $\phi = \pm\pi/6$. Note that, in this representation, classical geodesics of the billiard between two successive collisions are not straight lines since the centrifugal potential is stronger than in the Euclidean case. In what follows we restrict ourselves to the fundamental domain and choose basis functions that fulfill Dirichlet boundary conditions. These states are symmetric under particle exchange.

We are interested in highly excited eigenstates. These may be accurately computed numerically by using the scaling method developed in Ref. [18] and applied to a three-dimensional billiard by one of the authors [11]. This method works efficiently only when a suitable positive weight function is introduced in a boundary integral. To this purpose we note that the radial part of (4) looks similar to a four-dimensional Laplacian. Extending the results of Refs. [18,11] to four dimensions yields the appropriate weight function, which has a remarkably simple form in

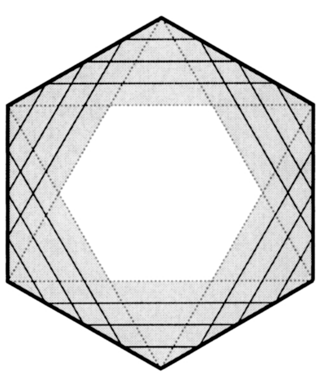

FIG. 1. The motion inside the collinear manifold corresponds to the motion inside a hexagonal billiard. The parabolic-elliptic family of periodic orbits is shaded, and five of its members are represented by lines.

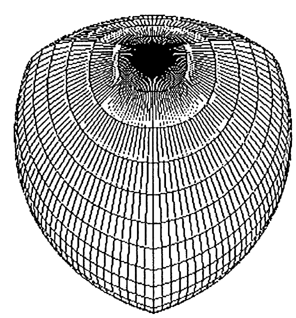

FIG. 2. Billiard shape after separating off the center of mass motion and rotational degree of freedom.

our coordinates; namely, we minimize the following functional:

$$f[\Psi_k] = \int_0^1 d\cos\theta \int_{-\pi/6}^{\pi/6} d\varphi\, \rho_B^4(\theta,\varphi) \times |\Psi_k(\rho_B(\theta,\varphi),\theta,\varphi)|^2,$$

where the wave function is expressed in terms of *scaling functions* (5), $\Psi_k = \sum_l c_{l,l_z}\psi_{k,l,l_z}$. Because of our particular choice of boundary conditions, we consider only the terms for which $l + l_z$ is *odd* and $l_z = 3m$, and truncate at $l = l_{\max} = ka/2 + \Delta l \approx ka/2$.

We have computed three stretches of highly excited states. They consist of 7430, 1813, and 2362 consecutive eigenstates with $120 < ka < 235$, $290 < ka < 300$, and $393 < ka < 400$, respectively. The last two stretches comprise levels with sequential quantum numbers around 20 000 and 45 000, respectively. The completeness of the series was checked by comparing the number of obtained eigenstates with the leading order prediction from the Weyl formula $\bar{d}(k) = c(24\pi^2)^{-1}(ak)^2,\ c \approx 0.513\,49$.

Figure 3 shows that the nearest neighbor spacing distribution agrees very well with RMT predictions already for the lower energy spectral stretch $120 \le ka \le 235$. The other series show well agreement, too. As for the long-range spectral correlations, the number variance $\Sigma^2(L)$ deviates from RMT predictions for interval length of more than ten mean level spacings which we believe is due to the parabolic-elliptic family of periodic orbits in the collinear manifold (Fig. 1). The deviation from RMT *decreases* with increasing k. For the highest spectral stretch ($ka \approx 400$) the number variance increases linearly, $\Sigma^2(L) \approx \Sigma^2_{\mathrm{GOE}}(L) + \varepsilon L$ up to $L \le 250$, with $\varepsilon \approx 0.04$. This finding is consistent with the model of a statistically independent fraction ε of strongly scarred states [11]. $\Sigma^2(L)$ reaches its maximum and begins to oscillate at the saturation length L^* which scales as $L^* \propto k^2$ in agreement with the prediction of Ref. [19].

The length spectrum $D(r)$, i.e., the cosine transform of the oscillatory part of the spectral density $d_{\mathrm{osc}}(k) = \sum_n \delta(k - k_n) - \bar{d}(k)$, gives further information about long-range spectral fluctuations. For finite stretches of consecutive levels in the interval $[k_1, k_2]$, one uses a Welsh window function $w(k;k_1,k_2) = (k_2 - k)(k - k_1)/[6(k_2 - k_1)^3]$ in the actual computation and obtains $D(l) = \int_{k_1}^{k_2} dk\, w(k;k_1,k_2)\cos(kr)d_{\mathrm{osc}}(k)$ (see, e.g., [6,11]). Figure 4 shows that orbits of length $r = \sqrt{2}\,a$ and its integer multiples cause dominant peaks in the length spectrum.

To investigate the observed deviations from RMT predictions in more detail, we consider the inverse participation ratio (IPR) of the wave functions in the angular momentum basis (5). This basis is particularly convenient and suitable since periodic orbits correspond to sets of isolated points within this representation. Let $c_{l,l_z}^{(n)}$ denote the expansion coefficients of nth eigenstate Ψ_{k_n}. We compute the IPR over a set of N consecutive eigenstates as $\mathrm{IPR}(l,l_z) \equiv N\sum_n |c_{l,l_z}^{(n)}|^4/(\sum_n |c_{l,l_z}^{(n)}|^2)^2$. The IPR is the first nontrivial moment of the distribution of the expansion coefficients $c_{l,l_z}^{(n)}$ and measures the inverse fraction of basis states that build up a wave function [3]. One has IPR $= 1$ for a wave function that has equal overlaps with all basis states and IPR $= N$ for a wave function that coincides with a basis state. The predicted RMT value for ideally quantum ergodic states is $\mathrm{IPR}_{\mathrm{GOE}} = 3$. Figure 5 shows the IPR for the two sets of eigenstates with $170 < k < 200$ and $290 < k < 300$, respectively. The agreement with RMT predictions is rather good in both cases. This confirms that the billiard under consideration is dominantly chaotic and ergodic. However, the IPR is enhanced in the region around $l = l_z \approx ka/3$, thus indicating some degree of localization. This is a robust phenomenon (present at all energy ranges), although the region of enhancement shrinks with increasing k. This finding is compatible with the expectation of uniform quantum ergodicity in the semiclassical limit. Note that the region $l \approx l_z$ corresponds to the

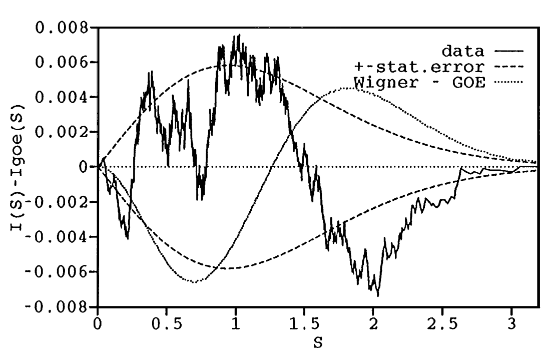

FIG. 3. Integrated nearest neighbor spacing distribution $I(S) = \int_0^S ds\,P(s)$ with the GOE value subtracted, $I(S) - I_{\mathrm{GOE}}(S)$, for the set of $N = 7430$ consecutive levels with $120 < k < 235$ (full line). The dashed curve is the estimated statistical error $\sigma = \sqrt{I(S)[1 - I(S)]/N}$ and the dotted curve is the difference for the commonly used Wigner surmise $I_{\mathrm{Wig}}(S) = 1 - \exp(-\pi S^2/4)$. Note that the deviations from RMT are *not visible* in the histogram for $P(S)$.

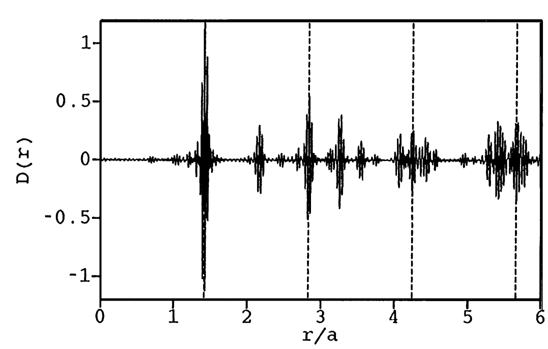

FIG. 4. Length spectrum $D(r)$ for the long spectral sequence with $120 < k < 235$. The dashed vertical lines denote the integer multiples of the period of the parabolic-elliptic family.

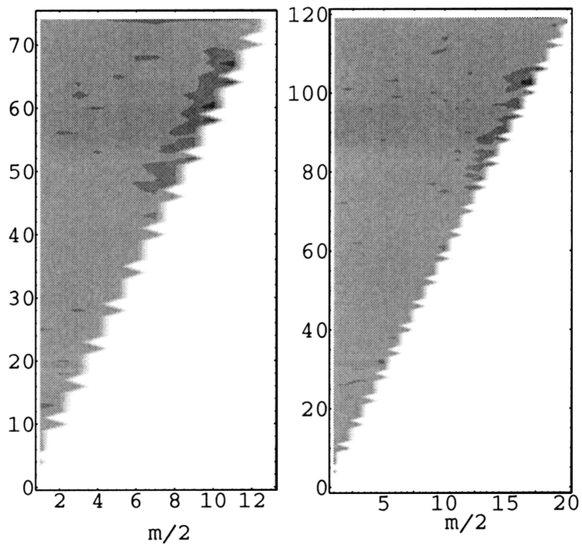

FIG. 5. IPR $(l, l_z = 3m)$, for 2052 states with $170 < ka < 200$ (left) and for 1813 states with $290 < ka < 300$ (right). Different levels of greyness are used for IPR values on consecutive intervals of width 0.5. The dominating light grey corresponds to the interval $[2.75, 3.25]$ around the RMT value 3; darker grey indicates some degree of localization.

vicinity of the collinear manifold. Note further that the orbits belonging to the parabolic-elliptic family depicted in Fig. 1 have length $\sqrt{2}\,a$ and angular momenta in the region $l/ka = l_z/ka \in (1/2\sqrt{6}, 1/\sqrt{6})$. This is precisely the region where the IPR exhibits its enhancement while the orbits' lengths coincide with the prominent peaks of the length spectrum in Fig. 4.

Thus, the deviations from RMT predictions observed for the spectrum and for the wave functions are associated with the family of parabolic-elliptic periodic orbits inside the collinear manifold. The special stability properties of this family lead to scars in the wave functions of the quantum system. This is an exciting new type of scars of invariant manifolds. It complements results previously found in helium [20], a three-dimensional billiard [11], and in interacting few-body systems [12]. Note that the family of parabolic bouncing ball orbits inside the collinear manifold does not cause statistically detectable scarring. The orbits of this family correspond to points in angular momentum space with $l = l_z < ka/2\sqrt{6}$ and do not exhibit an enhancement in the IPR since the classical motion is too unstable in their vicinity.

In summary, we have investigated an interacting three-body system realized as a convex billiard with no dispersing elements. Numerical results show that the classical dynamics is dominantly chaotic and no deviation from ergodic behavior is found. This is interesting with respect to recent efforts in constructing high-dimensional chaotic billiards. While the spectral fluctuations of the quantum system agree with RMT predictions on energy scales of a few mean level spacings, they exhibit interesting deviations on larger energy scales and in wave function intensities. These deviations are a manifestation of a new type of scars of a family of periodic orbits inside the collinear manifold.

We thank L. Kaplan for stimulating discussions and the Centro Internacional de Ciencias, Cuernavaca, Mexico, for its hospitality. This work was partly supported by the Department of Energy.

*Present address: Institute for Nuclear Theory, Department of Physics, University of Washington, Seattle, WA 98195. Email address: papenbro@phys.washington.edu

†Permanent address: Physics Department, Faculty of Mathematics and Physics, University of Ljubljana, Jadranska 19, 1111 Ljubljana, Slovenia. Email address: prosen@fiz.uni-lj.si

[1] O. Bohigas, M.-J. Giannoni, and C. Schmit, Phys. Rev. Lett. **52**, 1 (1984); T. Guhr, A. Müller-Groeling, and H. A. Weidenmüller, Phys. Rep. **299**, 189 (1998).

[2] E. J. Heller, Phys. Rev. Lett. **53**, 1515 (1984); E. Bogomolny, Physica (Amsterdam) **31D**, 169 (1988); M. V. Berry, Proc. R. Soc. London A **423**, 219 (1989); O. Agam and S. Fishman, Phys. Rev. Lett. **73**, 806 (1994).

[3] L. Kaplan, Phys. Rev. Lett. **80**, 2582 (1998); Nonlinearity **12**, R1 (1999).

[4] R. L. Weaver, J. Acoust. Soc. Am. **85**, 1005 (1989); C. Ellegaard *et al.*, Phys. Rev. Lett. **75**, 1546 (1995).

[5] J. U. Nöckel and A. D. Stone, Nature (London) **385**, 45 (1997); H. Alt *et al.*, Phys. Rev. Lett. **79**, 1026 (1997).

[6] H. Primack and U. Smilansky, Phys. Rev. Lett. **74**, 4831 (1995).

[7] T. Prosen, Phys. Lett. A **233**, 323 (1997).

[8] L. Bunimovich, G. Casati, and I. Guarneri, Phys. Rev. Lett. **77**, 2941 (1996); L. A. Bunimovich and J. Rahacek, Comun. Math. Phys. **189**, 729 (1997).

[9] O. Bohigas and H. A. Weidenmüller, Annu. Rev. Nucl. Part. Sci. **38**, 421 (1988); V. Zelevinsky, Annu. Rev. Nucl. Part. Sci. **46**, 237 (1996).

[10] T. Papenbrock and T. H. Seligman, Phys. Lett. A **218**, 229 (1996); A. López-Castillo, Phys. Rev. Lett. **77**, 4516 (1996).

[11] T. Prosen, Phys. Lett. A **233**, 332 (1997).

[12] T. Papenbrock, T. H. Seligman, and H. A. Weidenmüller, Phys. Rev. Lett. **80**, 3057 (1998).

[13] T. Papenbrock, Phys. Rev. C (to be published).

[14] M. Sieber and F. Steiner, Physica (Amsterdam) **44D**, 248 (1990).

[15] G. Bennetin, L. Galgani, and J. M. Strelcyn, Phys. Rev. A **14**, 2338 (1976).

[16] P. J. Richens and M. V. Berry, Physica (Amsterdam) **2D**, 495 (1981); B. Eckhardt, J. Ford, and F. Vivaldi, Physica (Amsterdam) **13D**, 339 (1984).

[17] H.-D. Gräf *et al.*, Phys. Rev. Lett. **69**, 1296 (1992).

[18] E. Vergini and M. Saraceno, Phys. Rev. E **52**, 2204 (1995).

[19] M. V. Berry, Proc. R. Soc. London A **400**, 229 (1985).

[20] D. Wintgen, K. Richter, and G. Tanner, Chaos **2**, 19 (1992).